

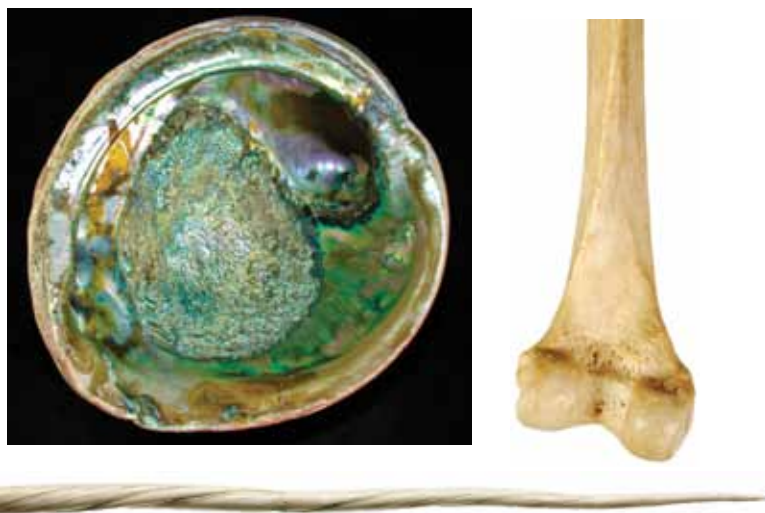
It's tough to be strong: Advances in bioinspired structural ceramic-based materials

By Michael M. Porter and Joanna McKittrick

Adapting biological processes to synthesize ceramic materials yields microstructures remarkably similar to natural materials with mechanical properties at least as good.

Biological materials science focuses on the structure–function–property–processing paradigm, a common theme in materials science. However, synthesis and growth of natural materials is quite different from that of synthetic materials. Almost all biological systems follow six fundamental design principles.^{1–3}

- **Water.** Although essential for biological systems, synthetic materials typically avoid water.
- **Cyclic, green process.** The life and decomposition cycles of biological systems occur at about standard temperature and pressure—300 K and 1 atm. Ceramic and metal processing involves high pressures and temperatures.
- **Local resources.** Biological systems use available organic (soft) and inorganic (hard) building blocks, made of carbon, nitrogen, oxygen, hydrogen, calcium, phosphorus, and sulfur, resulting in a vast array of hybrid systems. Synthetic materials require acquisition of resources.
- **Self-assembly.** A “bottom-up” process builds structural hierarchy across nanolength to macrolength scales. Engineers build structures from the top down.
- **Fitting form to function.** Biological systems grow, self-repair, and evolve as needed. Function dictates the organism's shape, not vice versa. This allows identification of the properties that have been optimized for a certain function.



Natural materials, such as nacre (top left), bone (top right), and narwhal tusk (bottom), suggest structures and processing approaches for new synthetic materials.

- **Hierarchical structures.** Efficiency and multifunctionality are organized over a range of scale levels (nanoscale to macroscale). Structure confers distinct and translatable properties from one level to the next and may be optimized for more than one function. For example, bone supports the body, stores ions, and produces marrow.

The idea behind bioinspired materials is to adapt the apparent effortless of biological systems to produce complex, multifunctional materials to make synthetic materials. Biological systems adapt to changing ambient conditions, continually refining and adjusting shape through chemical, cellular, and mechanical signaling. This requires a systems approach with the expertise of engineers as well as life scientists to develop materials with complex, hierarchical structures.

Two model structural materials—abalone nacre and bone—have exceptional mechanical properties designed for body support, as well as impact resistance (nacre) or blood flow and joint movement (bone). These properties result from highly ordered, structural alignment in multiple directions across several length scales. Bioinspired design seeks to mimic the nanostructural and microstructural features of natural materials to fabricate high-performance, multifunctional materials.

This review focuses on the development of cellular solids, tough ceramics, and hybrid composites inspired by bone and abalone nacre. These materials may be useful for a variety of applications ranging from load-bearing bone implants and lightweight structural composites to separation filters and catalyst supports.

Learning from bone and nacre

Bone and nacre are natural ceramic-based materials, containing organic matter, with extraordinary mechanical properties given their lightweight composition from locally available elements—calcium, phosphorous, carbon, oxygen, and hydrogen. They are stiff, strong, and tough—mechanical properties usually considered mutually exclusive⁴. The Ashby plot in Figure 1 compares the stiffness and toughness of bone and

nacre with several other natural materials.⁵ The plot shows these materials are surprisingly tough, considering their low density, high strength, and stiffness. These properties result from a hybrid, hierarchical design built by self-assembly from the molecular level up, resulting in anisotropic, hierarchical architectures.

Bone is about 65 wt% hydroxyapatite ($\text{Ca}_{10}(\text{PO}_4)_6(\text{OH})_2$) embedded in an organic matrix of type I collagen. Two main forms exist: cortical (or compact) and cancellous (or trabecular). At the microstructural level, osteons compose cortical bone and consist of dense (5–10 percent porosity), concentrically oriented lamellar sheets surrounding small vascular channels and lacuna spaces $\sim 10\text{--}50\ \mu\text{m}$ in diameter. Lamellar sheets, $3\text{--}7\ \mu\text{m}$ thick, have a “twisted plywood” architecture with fibers oriented at various angles.⁶ Each fiber is composed of several mineralized collagen fibrils $\sim 150\ \text{nm}$ in diameter and $5\text{--}10\ \mu\text{m}$ long. Each fibril consists of tropocollagen proteins and periodically spaced hydroxyapatite minerals with a characteristic periodicity of 67 nm. Figure 2(a) shows how the microstructure of cortical bone consists of layers (or lamellae) of aligned fibers that are oriented in successive rotations of $\sim 30^\circ$.^{7–9}

Cancellous bone, on the other hand, has a cellular structure (75–85 percent porosity) of trabecular struts surrounding large pores $100\text{--}500\ \mu\text{m}$ wide. Although morphologically similar to cortical bone at the submicrometer level, cancellous bone contains flat lamellar sheets, rather than cylindrical osteons. Mechanical loading mediates the growth of both bone types (i.e., bone grows in response to stress), which yields varying mechanical properties depending on location, age, sex, and physiology.

Compared with bone, nacre exhibits superior mechanical properties, primarily because it lacks porosity. Nacre is $\sim 95\ \text{wt}\%$ crystalline aragonite (CaCO_3) platelets embedded in an organic matrix of chitin and proteins.¹⁰ The inorganic-platelets and organic-matrix structure resembles a “brick-and-mortar” structure, with stacked aragonite “bricks” $\sim 0.5\ \mu\text{m}$ thick by $8\text{--}10\ \mu\text{m}$ wide “mortared” by organic layers $20\text{--}50\ \text{nm}$ thick (Figure

2(b)).¹⁰ Mineral bridges $25\text{--}55\ \text{nm}$ in diameter connect the platelets.¹¹ This organization of successive layers is a consequence of the nucleation and growth of aragonite crystals, leading to the formation of tiles aligned about the c -axis.¹² The platelets have a characteristic surface roughness caused by asperities $\sim 50\ \text{nm}$ wide and $30\ \text{nm}$ high.¹³ However, the platelets are not discrete tiles dispersed in a continuous organic matrix. Similar to bone, the organic and inorganic constituents are continuous, interpenetrating phases that grow concurrently.¹² Additional growth bands of organic layers $\sim 20\ \mu\text{m}$ thick, corresponding to periods of growth interruption, separate mesolayers $\sim 300\ \mu\text{m}$ wide.¹²

Several mechanisms across various length scales contribute to the excellent strength and toughness of bone and nacre. In cortical bone, extrinsic toughening occurs behind the crack tip at length scales $>1\ \mu\text{m}$,^{4,14} including crack deflection and twisting around osteons, uncracked-ligament bridging, collagen-fibril bridging, and constrained microcracking. Intrinsic toughening mechanisms in bone occur ahead of the crack tip at length scales $<1\ \mu\text{m}$ ^{4,14} and include hidden length sacrificial bonding, microcracking, fibrillar sliding, and molecular uncoiling. In nacre, the brick-and-mortar structure deflects

crack propagation, leading to failure via delamination, tile pullout, or tile fracture.^{15,16} As stress accumulates, the organic matrix dissipates energy, acting as a tough, viscoelastic glue.^{13,17} The mineral bridges resist intertile shearing (tile pullout) and tensile failure (tile fracture), acting as reinforcing struts to give nacre its strength and stiffness. The surface asperities prevent excessive sliding between adjacent platelets, further protecting nacre from fracture by delamination or tile pullout.^{13,17} Other toughening mechanisms in nacre include platelet interlocks (waviness) as well as rotation, sliding, and organic bridging between nanograins.^{15,16}

On a more fundamental level, the microstructural anisotropy found in cortical bone and nacre provides these materials their high mechanical properties (Table 1). The high, yet anisotropic, compressive strengths relate directly to the

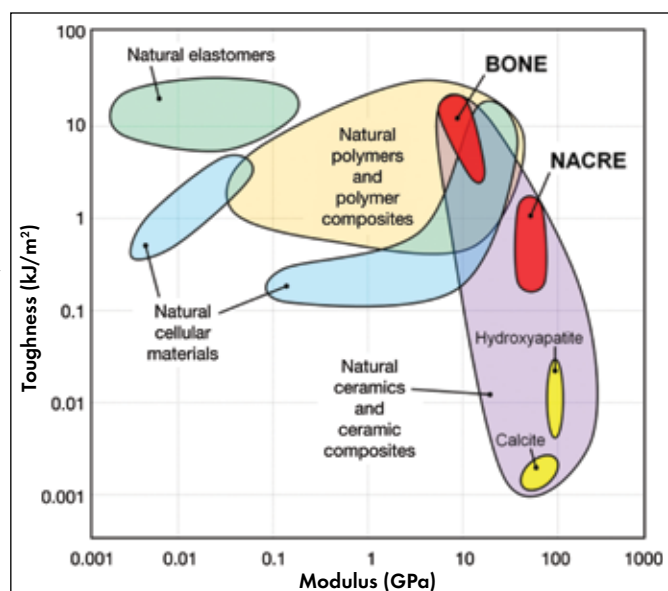


Figure 1. Ashby plot comparing toughness and modulus. Bone and nacre are tough materials despite their low density.⁵

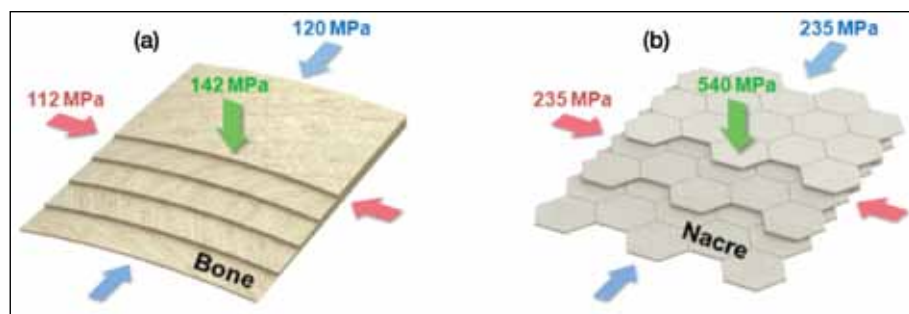


Figure 2. Compressive strengths reflect microstructural anisotropies. (a) Cortical bone has a “twisted plywood” lamellar microstructure. (b) Abalone nacre microstructure follows a “brick-and-mortar” morphology.^{8,9}

It's tough to be strong: Advances in bioinspired structural ceramic-based materials

orientation, alignment, and uniformity of the layered microstructures in bone and nacre (Figure 2).

Engineering bioinspired materials

The natural world provides many examples of cellular structures: trabecular bone, plant stems (e.g., wood), cuttlefish bones, corals, sponges, sea urchin spines, horseshoe crab exoskeletons, feathers, porcupine quills, and bird beak interiors. An interconnected network of struts and plates form the faces of the cell walls in cellular solids. The cells tend to align for maximum mechanical efficiency. Therefore, many cellular solids develop anisotropically as they respond to load orientations. For example, the compressive strength of a trabecular femur head is much higher in the direction of maximum load than in the transverse directions.¹⁸ Research shows that the elastic modulus and strength of an open cell porous material are strong functions of density.¹⁸ Cellular solids are of interest in the biomedical field as scaffolds for bony (osseointegration) or cellular ingrowth. Therefore, mechanical integrity is important.

Emulating the intricate organization of the molecular, nano-, micro-, and macrostructures found in nature may be the key to developing higher performance synthetic materials. Using advanced synthetic materials, such as alumina, zirconia, polymethylmethacrylate (PMMA), and epoxy, rather than nature's relatively weak constituents, such as hydroxyapatite, aragonite (CaCO_3), collagen, and chitin, it becomes possible to engineer bioinspired materials with hybrid, hierarchical architectures that outperform their biological counterparts. For example, according to the rule of mixtures, the global mechanical properties (X) of a hybrid composite material depend on the properties (X_i) and fractions (ϕ_i) of the individual parts (i):

$$X = \sum \phi_i X_i.$$

However, most biological materials do not follow the rule of mixtures and exhibit higher than expected mechanical properties.¹⁹ For instance, two common modes of failure in platelet-reinforced composites are platelet frac-

ture (brittle failure) and platelet pullout (ductile failure).²⁰ Both bone and nacre have optimized interfacial adhesion between the stiff inorganic platelets and ductile organic matrix, such that ductile failure occurs just before brittle failure. This adaptation, combined with structural hierarchy, provides bone and nacre extremely high flaw tolerance and fracture toughness^{20,21}—better than most synthetic materials.

Bioinspired ceramic-based materials

Drawing inspiration from hard biological materials, many research groups in the past decade have engineered extremely strong, stiff, and tough ceramic-based materials by various nature-inspired processes to produce thin films, porous scaffolds, or bulk composites. Table 1 compares the properties of bone and nacre with selected bioinspired materials, which were selected because they mimic, or draw inspiration from, one or more of the nanostructural or microstructural features that provide bone and nacre their extraordinary mechanical properties.

Thin films

Inspired by nacre, thin film bottom-up fabrication techniques exploit chemical, physical, electrical, or mechanical forces to drive assembly of synthetic building blocks. Methods include layer-by-layer self-assembly, enzyme- and peptide-mediated synthesis, biomineralization, centrifugation, evaporation or vacuum filtration, solution casting, chemical bath or electrophoretic deposition, ion beam sputtering, and morpho-synthesis. Most of these syntheses occur near room temperature and in an aqueous environment.

Organic constituents control and regulate size, morphology, orientation, texture, and organization of mineral crystals in biological systems. Langmuir–Blodgett films, reverse micelles, liquid crystals, and self-assembled monolayers (SAMs) have mimicked successfully chemistries of biological proteins that promote nucleation of inorganic crystals. The SAM approach has been most effective for nucleating crystals with controlled orientation and polymorph. SAM molecules have the general formula RSiX_3 ,

where R is an organic functional group and X is typically an alkoxide or halide. One end of the SAM molecule attaches to the substrate and the other functional end promotes nucleation of inorganic crystals. Tailoring the functional group allows for deposition of continuous or patterned ceramic thin films.²² Crystalline single-metal oxides can be deposited at temperatures $<100^\circ\text{C}$, making this an attractive method for further development. However, crystalline multiconstituent metal oxides are difficult to produce using this method.

Enzymes catalyze chemical reactions such as hydrolysis, reduction–oxidation, and elimination of specific functional groups in living matter. They also can be used for site selective oxide, hydroxide, carbonate, and phosphate deposition at low temperatures. For example, the enzyme silicatein- α promotes biosynthesis of SiO_2 in sponges and diatoms and can be isolated and cloned from glass sponges. It also can catalyze nucleation of ceramic films, particles, and nanowires of TiO_2 , ZrO_2 , SnO_2 , and CaTiO_3 .²³ Peptides, proteins, polyamides, and amino acids—acting as a catalyst or template to control the morphology, polymorph, and orientation—induce nucleation of TiO_2 . Catalyzed hydrolysis of phosphate esters by alkaline phosphatase produces patterned thin films of hydroxyapatite on collagen substrates.²⁴ The above methods produce a thin layer, prompting researchers to pursue other methods to attempt to duplicate the layered microstructure to macrostructure of bone and nacre films.

A significant early attempt to develop nacre-like films deposited sequential layers of montmorillonite (MTM) clay platelets and poly(diallyldimethylammonium chloride) polyelectrolytes using a surfactant-mediated self-assembly approach.²⁵ The films had ultimate tensile strengths up to 109 MPa and Young's moduli up to 13 GPa, similar to the properties of nacre and cortical bone, respectively. A similar layer-by-layer approach fabricated MTM/poly(vinyl alcohol) nanocomposites closely resembling nacre's brick-and-mortar microstructure and formed optically transparent multilayer composites with an unsurpassed stiffness

compared with similar nanocomposite films.²⁶ A sequence of Al₂O₃/chitosan films produced with a bottom-up spin-coating technique produced more ductility and flaw tolerance than prior works, with observed ultimate tensile strains up to 21 percent.²¹ An alternative approach used ecofriendly vacuum filtration, similar to papermaking, to fabricate high-strength and high-stiffness MTM/PVA composites with varying optical transparencies, as well as gas barrier and fire-resistant properties.²⁷ (See Table 1 for property data.)

Thin films have outstanding mechanical properties and unique functionalities, but they are, in fact, thin—less than 1 mm. Although they are impractical for many structural applications, films can be used as hard coatings, displays, sensors, and optical equipment.

Porous scaffolds

Porous scaffolds that mimic bone are ideal for tissue engineering applications, such as load-bearing bone implants that promote tissue ingrowth or other applications requiring high porosity and reasonable mechanical strength. Researchers report many different methods to emulate the trabecular architecture of cancellous bone including direct foaming²⁸ and polymer sponge replication.²⁹ However, mimicking cancellous bone is not ideal for load-bearing applications because of its high porosity, near isotropic structure, and poor mechanical properties. Instead, highly anisotropic scaffolds with unidirectionally aligned pores have shown great potential for load-bearing applications.^{30,31} For example, researchers made porous scaffolds by dipping polyurethane foams repeatedly into ZrO₂ or hydroxyapatite slurries, drying, and then burning out the foam. The ZrO₂ scaffold achieved high compressive strength (35 MPa), whereas the strength of the hydroxyapatite scaffold was ~4 MPa.²⁹ Another interesting method uses the unidirectional porosity of wood as a template to fabricate anisotropic hydroxyapatite scaffolds, following a series of chemical treatments.³² The method achieved optimal pore-size distribution (100–300 μm) required for the migration and proliferation of osteoblasts (bone synthesizing cells). However, the

mechanical properties were poor compared with other unidirectionally aligned porous scaffolds (Table 1).

The advent of additive manufacturing enables fabrication of a variety of porous scaffolds with designer architectures. This technique has gained tremendous attention in the medical industry as an efficient means to customize scaffolds for biomedical implants. Direct ink-write assembly has been used to form bioactive glass scaffolds with regular pore spacing of 500 μm and cell walls 100 μm thick.³¹

High compressive strength and modulus were reached (136 MPa and 2 MPa) with a porosity of 60 percent, which is within the range of cancellous bone (Table 1). The scaffolds promoted nucleation of hydroxyapatite after soaking in simulated body fluid for two weeks, indicating that the material is ideal for osseointegration. However, the mechanical properties of 3D-printed parts depend on the formation and resolution of the layers (highest resolutions are ~10 μm). Ultimately, the interface between layers is the weakest point of the structure and may lead to catastrophic crack initiation, propagation, and subsequent failure. Because of its high cost, high energy consumption, extended fabrication times, limited material availability, restricted workspace, and poor material properties, 3D printing is not the most economical means to develop high-performance scaffolds.

Until additive manufacturing technologies improve, other methods to fabricate high-strength, porous scaffolds are preferable. Currently, one of the best methods for forming aligned porous scaffolds is freeze casting from a (usually) aqueous-based slurry. Adding

surfactants and binders improves particle dispersion and as-cast strength. With this method, the slurry is poured into a mold set on a freezing surface. The freezing surface is controlled, such that a thermal gradient leads to the directional solidification of the slurry. Constitutional supercooling sets up instabilities on the liquid–solid interface as the freezing front advances in the slurry. These perturbations (instabilities) crystallize into ice dendrites that shoot out into the liquid. The ice crystals expel particles between dendrites, thereby forming a lamellar structure. Finally, the frozen slurry is freeze-dried and sintered to form a structurally robust scaffold. Processing variables include volume fraction of solid powder, cooling rate, and liquid properties, such as viscosity. A polymer or metal can be infiltrated into these scaffolds to form lamellar composites.

Bulk composites

Because of their large macrostructures and scalability, bulk ceramic-based composites are, quite possibly, the most versatile and high performance bioin-

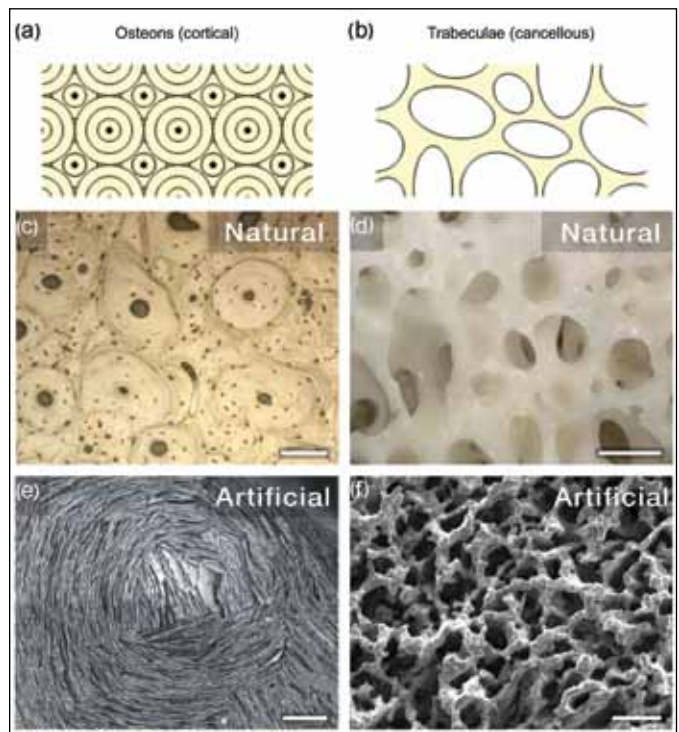


Figure 3. Natural and artificial osteonal and trabecular bone structures. (a–b) Schematic osteonal and trabecular bone architectures; (c) natural osteons in cortical bone; (d) natural trabecular struts in cancellous bone; (e) aligned freeze cast microstructure mimics osteonal bone architecture.³⁸ (f) artificial scaffold mimics trabecular bone architecture. Scale bars: (c) 100 μm; (d) 500 μm; (e) 500 μm; (f) 25 μm.

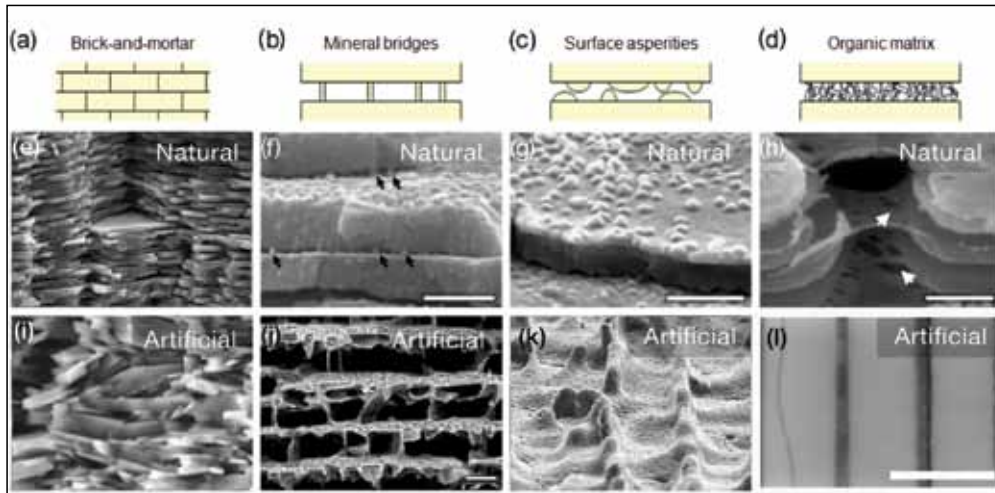


Figure 4. Nacre microstructure types and schematics show different architectures. The middle row shows natural nacre microstructures. The bottom row shows artificial nacre microstructures. (a, e, i) brick-and-mortar; (b, f, j) mineral bridges; (c, g, k) surface asperities; and (d, h, l) organic matrix. Scale bars: (f) 500 nm; (g) 500 nm; (h) 1 μm ; (j) 20 μm ; (l) 1 μm .

spired materials. Promising techniques for making composites with enhanced mechanical properties include infiltrating ceramic scaffolds with polymers or metals and aligning ceramic microstructures with external forces. Variations of polymer or metal infiltration techniques into ceramic scaffolds include melt immersion, solvent evaporation, in-situ polymerization, particle centrifugation, and chemical vapor deposition.

Table 1 compares flexural strength and fracture toughness for crack initiation of several high-toughness Al_2O_3 -based composites. Pressure sintering and infiltrating with PMMA were used to form freeze-cast Al_2O_3 scaffold composites that resemble the brick-and-mortar structure of nacre with features such as mineral bridges extending from one lamella to another and surface roughness (asperities) on the ceramic phase.³³ Infiltrating molten Al-Si alloys into freeze-cast Al_2O_3 scaffolds increased flexural strength (up to 328 MPa) and toughness (up to 8.3 $\text{MPa}\cdot\text{m}^{1/2}$).³⁴ However, polymeric or metallic phases in the Al_2O_3 -based composites may be undesirable for certain applications, such as high-temperature environments. Therefore, freeze casting and densification with pressurized spark plasma sintering was used to develop $\text{Al}_2\text{O}_3/\text{SiO}_2/\text{CaO}$ composites. These composites exhibited the highest combination of strength (470 MPa) and toughness (6.2 $\text{MPa}\cdot\text{m}^{1/2}$) yet to be

reported for a fully ceramic material.³⁵ Capitalizing on freeze casting to control growth of ice crystals provides these materials microstructural alignment and outstanding combinations of strength and toughness. Similar to bone and nacre, these composites employ several fracture resistance mechanisms.

Yet another technique used low magnetic fields to align Al_2O_3 platelets in polymer matrices.^{36,37} The aligned microstructures increased flexural modulus, strength, and fracture toughness significantly compared with identical composites without magnetic alignment.³⁷ However, these composites are limited by the low achievable volume fraction and discontinuity of ceramics platelets embedded in a continuous polymer matrix.

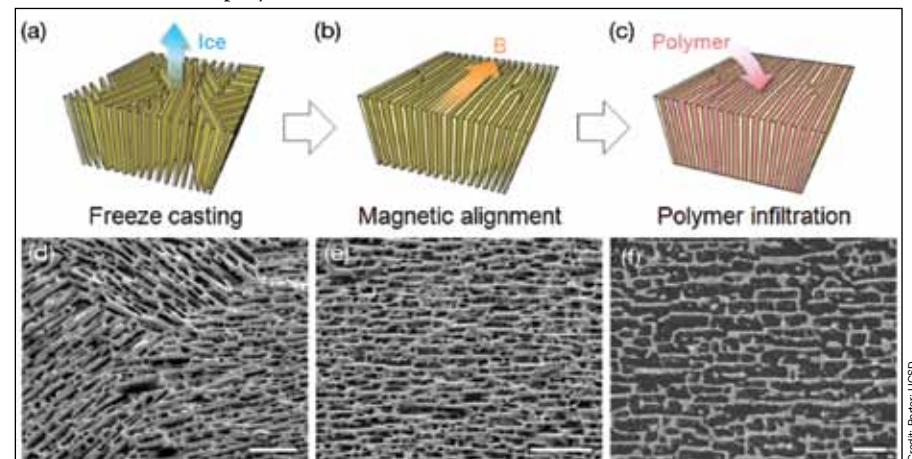


Figure 5. Microstructure alignment with applied magnetic field during freeze casting. (a) Freeze cast, (b) magnetic alignment, and (c) polymer infiltration to produce ceramic-based porous scaffolds and hybrid composites. (d, e) ZrO_2 scaffolds and (f) ZrO_2 -epoxy composites fabricated by the respective techniques. All scale bars are 100 μm .

Inspirations from biological structures

Figure 3 shows two artificial materials inspired by bone that mimic the microstructures of osteons (Figures 3(a) and (c)) and trabeculae (Figures 3(b) and (d)). Figure 3(e) shows an artificial osteon-like architecture produced by freeze casting in a mold with a patterned bottom surface to promote alignment of the ceramic particles.³⁸ The artificial trabecular scaffold shown in Figure 3f was also fabricated by freeze casting using a high viscosity water-based freezing vehicle.

Figure 4 juxtaposes schematics and micrographs of natural abalone nacre (Figures 4(a)–(h)) with several bioinspired materials that mimic the microstructural features of nacre (Figures 4(i)–(l)). In the first column of Figure 4 (parts (a), (e), and (i)), the strong and tough ceramics developed by Bouville et al.³⁵ are compared with natural nacre. These ceramics had extremely high mechanical properties (Table 1) and mimicked almost all microstructural features of nacre on equivalent length scales, including the brick-and-mortar architecture, platelets, mineral bridges, and surface asperities. The next three columns of Figure 4 compare natural and artificial mineral bridges (Figure 4(b), (f), (j)), surface asperities (Figure 4(c),

Table 1. Structural and mechanical properties of bone and nacre compared to selected bioinspired thin films, porous scaffolds, and bulk composites.

		Material composition	Total porosity (%)	Young's modulus (GPa)	Ultimate strength* (MPa)	Ultimate strain (%)	Fracture toughness (MPa·m ^{1/2})
Natural Materials	Bone (cancellous) ⁴⁵⁻⁴⁷	HA/collagen	> 30	0.001-0.5	0.2-116 ^c	0.3-3	---
	Bone (cortical) ^{45,48,49}	HA/collagen	< 30	6-28	10-172 ^t	0.9-2	2-11
					106-283 ^c		
					157-238 ^b		
	Abalone nacre ^{17,50,51}	CaCO ₃ /chitin	---	10-147	3-170 ^t	0.2-2	3-9
					235-540 ^c		
					177-197 ^b		
Thin films ^a	Podsiadla et al. ²⁶	MTM/PVA	---	106	400 ^t	0.33	---
	Bonderer et al. ²¹	Al ₂ O ₃ /chitosan	---	9.6	315 ^t	21	---
	Walther et al. ²⁷	MTM/PVA	---	45.6	248 ^t	0.9	---
Porous Scaffolds ^b	Almirall et al. ²⁸	HA	51-66	---	1.2-4.3 ^c	---	---
	Kim et al. ²⁹	ZrO ₂	74-92	---	1.6-35 ^c	---	---
	Tampieri et al. ³²	HA	70-85	---	2.5-4 ^c	---	---
	Fu et al. ³¹	Glass	60-80	---	40-136 ^c	---	---
	Deville et al. ³⁰	HA	47-64	---	16-145 ^c	---	---
Bulk Composites ^c	Estili et al. ⁴⁴	Al ₂ O ₃ /CNT	---	---	404 ^b	---	4.62
	Munch et al. ³³	Al ₂ O ₃ /PMMA	---	---	210 ^b	---	5.1
	Launey et al. ³⁴	Al ₂ O ₃ /Al/Si	---	---	328 ^b	---	8.3
	Bouville et al. ³⁵	Al ₂ O ₃ /SiO ₂ /CaO	---	290	470 ^b	---	6.2
	Libanori et al. ³⁷	Al ₂ O ₃ /Epoxy	---	16.6	180 ^b	---	2.56

^aHighest reported values for Young's modulus, ultimate tensile strength, and ultimate strain to failure; ^bRange of values for the total porosity and ultimate compressive strength; ^cHighest reported values for Young's modulus (flexure), ultimate bend strength, and fracture toughness for crack initiation; *Legend: C: compressive; T: tensile; B: bend.

(g), (k)), and organic matrices (Figure 4(d), (h), (l)).^{33,39,40} The artificial mineral bridges and surface asperities were fabricated by freeze casting,³³ and the artificial nacre was produced by sequential deposition of ZrN and PMMA.⁴¹ Although all features occur on different length scales in the natural and artificial materials (on the order of ~50 nm for the natural and 500–5000 nm for the artificial), their mechanical functions are the same. The mineral bridges and surface asperities add strength and stiffness, resistance to tensile fracture, and intertile shearing. The organic matrix adds toughness and dissipates energy that accumulates between adjacent lamellae under stress.

The micrographs in Figures 3 and 4 show different processing techniques used to synthesize bioinspired materials that mimic structural features of bone and abalone nacre, leading to outstanding mechanical properties that either match or surpass those of their natural counterparts. Ceramic microstructures resulting from freeze casting can be further manipulated by applying an external magnetic or electric field. Figure 5 provides an overview of magnetic-field-assisted freeze casting, and Figure 6 shows an example of a rotating magnetic field used to make helix-reinforced structures inspired by narwhal tusks. Freeze casting efficiently

fabricates porous ceramic scaffolds with unidirectionally aligned pores, perpendicular to the direction of ice growth (Figure 5(a)). Applying magnetic fields during freeze casting imposes a second order of microstructural alignment, parallel to the magnetic field direction and perpendicular to the ice growth direction (Figure 5(b)). Finally, infiltrating the bialigned porous scaffolds with a second phase, such as a polymer, yields bulk hybrid composite materials with designer architectures and enhanced mechanical properties (Figure 5(c)). With a static magnetic field, the resulting scaffolds have more than two times the strength in the transverse (magnetic field) direction, without significantly affecting the strength in the longitudinal (ice growth) direction.⁴² With a rotating magnetic field, the polymer-infiltrated composites have enhanced torsional properties over those produced without the field.⁴³

Summary

Structural bioinspired materials development is an active area of investigation and has led to ceramic thin films, porous scaffolds, and composites with unique and superior mechanical properties. Thin films are applied as hard coatings, and the most successful films are synthesized with self assembled monolayers of organic molecules that act as catalysts and templates for the nucleation and

growth of the inorganic phase. Porous scaffolds have application as biomedical implants, especially in bone repair and replacement. Because living bone tissue adapts its structure to maximize strength and stiffness in the load bearing direction, synthetic scaffolds must have some degree of anisotropy. The most successful scaffolds are formed from particle infused sacrificial templates, 3D printing, and freeze casting. Fabrication of composites that mimic the structure of nacre is achieved mainly by freeze casting and subsequent polymer or metal infiltration of the aligned porous scaffolds, which leads to extremely strong and tough laminates, with fracture toughness values that exceed any monolithic ceramic. New developments involve field-assisted freeze casting, which can strengthen the scaffold in multiple directions.

It is not enough to simply examine a biological material and attempt to duplicate its structure. Rather, functional aspects of the constituents and the microstructural details that result in strength and toughness must be understood. Successful duplication of the important features results in new materials with exceptional properties.

Acknowledgements

We thank Marc Meyers at University of California, San Diego, and Antoni Tomsia at the Lawrence Berkeley

It's tough to be strong: Advances in bioinspired structural ceramic-based materials

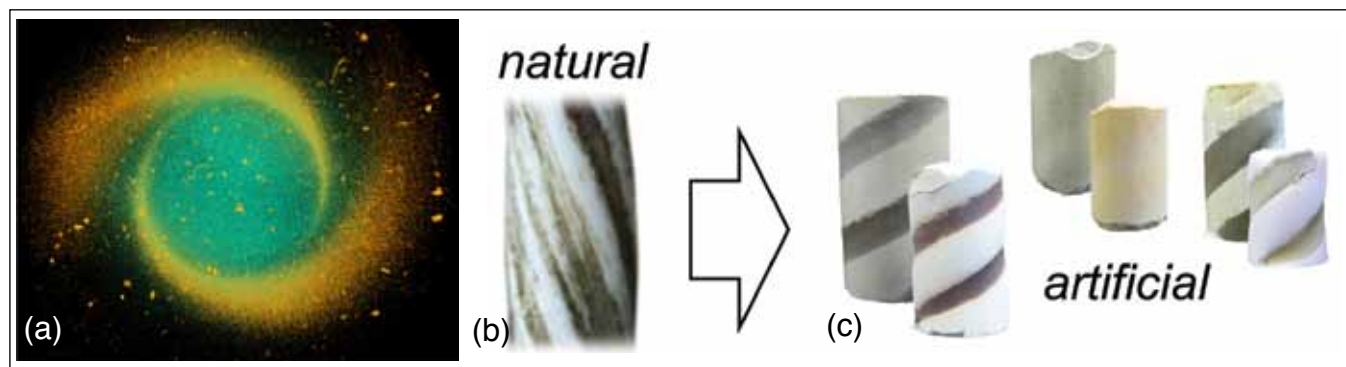


Figure 6. The helical structure of a narwhal tusk was replicated by applying a rotating magnetic field during freeze casting. (a) Micro-computed tomographic image of the top view of a sintered TiO₂ scaffold; (b) section of a narwhal tusk; (c) artificial scaffolds formed by magnetic field-assisted freeze casting.

National Laboratory for helpful discussions. The National Science Foundation Ceramics Program Grant No. 1006931, and a UCS, Academic Senate Bridge Grant (2013–2014) funded this work.

About the authors

Michael M. Porter is a doctoral researcher in the materials science and engineering program of the mechanical and aerospace engineering department at the UCSD. Joanna McKittrick is professor of mechanical and aerospace engineering at UCSD. Contact Joanna McKittrick at jmckittrick@ucsd.edu.

References

¹P. Fratzl and R. Weinkamer, "Nature's hierarchical materials," *Prog. Mater. Sci.*, **52**, 1263–334 (2007).

²M.A. Meyers, P.Y. Chen, A.Y.M. Lin, and Y. Seki, "Biological materials: Structure and mechanical properties," *Prog. Mater. Sci.*, **53**, 1–206 (2008).

³P.Y. Chen, J. McKittrick, and M.A. Meyers, "Biological materials: Functional adaptations and bioinspired designs," *Prog. Mater. Sci.*, **57**, 1492–704 (2012).

⁴R.O. Ritchie, "The conflicts between strength and toughness," *Nat. Mater.*, **10**, 817–22 (2011).

⁵U.G.K. Wegst and M.F. Ashby, "The mechanical efficiency of natural materials," *Philos. Mag.*, **84**, 2167–81 (2004).

⁶S. Weiner and H.D. Wagner, "The material bone: Structure mechanical function relations," *Annu. Rev. Mater. Sci.*, **28**, 271–98 (1998).

⁷S. Weiner, W. Traub, and H.D. Wagner, "Lamellar bone: Structure–function relations," *J. Struct. Biol.*, **126**, 241–55 (1999).

⁸P.Y. Chen, A.Y.M. Lin, Y.S. Lin, Y. Seki, S.G. Stokes, J. Peyras, E.A. Olevsky, M.A. Meyers, and J. McKittrick, "Structure and mechanical properties of selected biological materials," *J. Mech. Behav. Biomed. Mater.*, **1**, 208–26 (2008).

⁹E. Novitskaya, P.-Y. Chen, S. Lee, A. Castro-Ceseña, G. Hirata, V.A. Lubarda, and J. McKittrick, "Anisotropy in the compressive mechanical properties of bovine cortical bone and the mineral and protein constituents," *Acta Biomater.*, **7**, 3170–77 (2011).

¹⁰A.P. Jackson, J.F.V. Vincent, and R.M. Turner, "The mechanical design of nacre," *Proc. R. Soc. London, B-Biol. Sci.*, **234**, 415 (1988).

¹¹K. Gries, R. Kröger, C. Kübel, M. Schowalter, M. Fritz, and A. Rosenauer, "Correlation of the orientation of stacked aragonite platelets in nacre and their connection via mineral bridges," *Ultramicroscopy*, **109**, 230–36 (2009).

¹²A. Lin and M.A. Meyers, "Growth and structure in abalone shell," *Mater. Sci. Eng., A*, **390**, 27–41 (2005).

¹³M.A. Meyers, A.Y.-M. Lin, P.-Y. Chen, and J. Muyco, "Mechanical strength of abalone nacre: Role of the soft organic layer," *J. Mech. Behav. Biomed. Mater.*, **1**, 76–85 (2008).

¹⁴M.E. Launey, M.J. Buehler, and R.O. Ritchie, "On the mechanistic origins of toughness in bone"; pp. 25–53 in *Annual Review of Materials Research*, Vol 40. Edited by D.R. Clarke, M. Ruhle, and F. Zok. Annual Reviews, Palo Alto, Calif., 2010.

¹⁵H. Kakisawa and T. Sumitomo, "The toughening mechanism of nacre and structural materials inspired by nacre," *Sci. Technol. Adv. Mater.*, **12**, 064710 (2011).

¹⁶J.Y. Sun and B. Bhushan, "Hierarchical structure and mechanical properties of nacre: A review," *RSC Adv.*, **2**, 7617–32 (2012).

¹⁷A.Y.-M. Lin, P.-Y. Chen, and M.A. Meyers, "The growth of nacre in the abalone shell," *Acta Biomater.*, **4**, 131–38 (2008).

¹⁸L.J. Gibson, M.F. Ashby, and B.A. Harley, *Cellular materials in nature and medicine*. Cambridge University Press, Cambridge, U.K., 2010.

¹⁹M.A. Meyers, J. McKittrick, and P.-Y. Chen, "Structural biological materials: Critical mechanics–materials connections," *Science*, **339**, 773–79 (2013).

²⁰A.R. Studart, "Towards high-performance bioinspired composites," *Adv. Mater.*, **24**, 5024–44 (2012).

²¹L.J. Bonderer, A.R. Studart, and L.J. Gauckler, "Bioinspired design and assembly of platelet-reinforced polymer films," *Science*, **319**, 1069–73 (2008).

²²Y. Gao and K. Koumoto, "Bioinspired ceramic thin-film processing: Present status and future perspectives," *Cryst. Growth Des.*, **5**, 1983–2017 (2005).

²³R. Andre, M.N. Tahir, F. Natalio, and W. Tremel, "Bioinspired synthesis of multifunctional inorganic and bio-organic hybrid materials," *FEBS J.*, **279**, 1737–49 (2012).

²⁴H. Unuma, Y. Matsushima, and T. Kawai, "Enzyme-mediated synthesis of ceramic materials," *J. Ceram. Soc. Jpn.*, **119**, 623–30 (2011).

²⁵Z.Y. Tang, N.A. Kotov, S. Magonov, and B. Ozturk, "Nanostructured artificial nacre," *Nat. Mater.*, **2**, 413–18 (2003).

²⁶P. Podsiadlo, A.K. Kaushik, E.M. Arruda, A.M. Waas, B.S. Shim, J.D. Xu, et al., "Ultrastrong and stiff layered polymer nanocomposites," *Science*, **318**, 80–83 (2007).

²⁷A. Walther, I. Bjurhager, J.M. Malho, J. Pere, J. Ruokolainen, L.A. Berglund, and O. Ikkala, "Large-area, lightweight, and thick biomimetic composites with superior material properties via fast, economic, and green pathways," *Nano Lett.*, **10**, 2742–48 (2010).

²⁸A. Almirall, G. Larrecq, J.A. Delgado, S. Martinez, J.A. Planell, and M.P. Ginebra, "Fabrication of low-temperature macroporous hydroxyapatite scaffolds by foaming and hydrolysis of an alpha-TCP paste," *Biomaterials*, **25**, 3671–80 (2004).

²⁹H.W. Kim, S.Y. Lee, C.J. Bae, Y.J. Noh, H.E. Kim, H.M. Kim, and J.S. Ko, "Porous ZrO₂ bone scaffold coated with hydroxyapatite with fluorapatite intermediate layer," *Biomaterials*, **24**, 3277–84 (2003).

³⁰S. Deville, E. Saiz, and A.P. Tomsia, "Freeze casting of hydroxyapatite scaffolds for bone tissue engineering," *Biomaterials*, **27**, 5480–89 (2006).

³¹Q.A. Fu, E. Saiz, and A.P. Tomsia, "Bioinspired strong and highly porous glass scaffolds," *Adv. Funct. Mater.*, **21**, 1058–63 (2011).

³²A. Tampieri, S. Sprio, A. Ruffini, G. Celotti, I.G. Lesci, and N. Roveri, "From wood to bone: Multistep process to convert wood hierarchical structures into biomimetic hydroxyapatite scaffolds for bone tissue engineering," *J. Mater. Chem.*, **19**, 4973–80 (2009).

³³E. Munch, M.E. Launey, D.H. Alsem, E. Saiz, A.P. Tomsia, and R.O. Ritchie, "Tough, bio-inspired hybrid materials," *Science*, **322**, 1516–20 (2008).

³⁴M.E. Launey, E. Munch, D.H. Alsem, E. Saiz, A.P. Tomsia, and R.O. Ritchie, "A novel biomimetic approach to the design of high-performance ceramic–metal composites," *J. R. Soc. Interface*, **7**, 741–53 (2010).

³⁵F. Bouville, E. Maire, S. Meille, B. Van de Moortele, A.J. Stevenson, and S. Deville, "Strong, tough, and stiff bioinspired ceramics from brittle constituents," *Nat. Mater.*, **13**, 508–14 (2014).

³⁶R.M. Erb, R. Libanori, N. Rothfuchs, and A.R. Studart, "Composites reinforced in three dimensions by using low magnetic fields," *Science*, **335**, 199–204 (2012).

³⁷R. Libanori, R.M. Erb, and A.R. Studart, "Mechanics of platelet-reinforced composites assembled using mechanical and magnetic stimuli," *ACS Appl. Mater. Interfaces*, **5**, 10794–805 (2013).

³⁸S. Deville, E. Saiz, R.K. Nalla, and A.P. Tomsia, "Freezing as a path to build complex composites," *Science*, **311**, 515–18 (2006).

³⁹M.E. Launey, E. Munch, D.H. Alsem, H.B. Barth, E. Saiz, A.P. Tomsia, and R.O. Ritchie, "Designing highly toughened hybrid composites through nature-inspired hierarchical complexity," *Acta Mater.*, **57**, 2919–32 (2009).

⁴⁰S. Deville, "Freeze-casting of porous ceramics: A review of current achievements and issues," *Adv. Eng. Mater.*, **10**, 155–169 (2008).

⁴¹G.A. Hirata, S.P. Diaz, P.-Y. Chen, M.A. Meyers, and J. McKittrick, "Bioinspired inorganic/polymer thin films," *Materials Research Society Symposium Proceedings*, 1239, VV01-05 (8 pp) (2010).

⁴²M.M. Porter, M. Yeh, J. Strawson, T. Goehring, S. Lujan, P. Siripapasotorn, M.A. Meyers, and J. McKittrick, "Magnetic freeze casting inspired by nature," *Mater. Sci. Eng. A*, **556**, 741–50 (2012).

⁴³M.M. Porter, M.A. Meyers, and J. McKittrick, unpublished.

⁴⁴M. Estili, A. Kawasaki, and Y. Sakka, "Highly concentrated 3D macrostructure of individual carbon nanotubes in a ceramic environment," *Adv. Mater.*, **24**, 4322 (2012).

⁴⁵L.J. Gibson, "The mechanical behavior of cancellous bone," *J. Biomech.*, **18**, 317 (1985).

⁴⁶S.A. Goldstein, "The mechanical properties of trabecular bone—Dependence on anatomic location and function," *J. Biomech.*, **20**, 1055–61 (1987).

⁴⁷L. Rohl, E. Larsen, F. Linde, A. Odgaard, and J. Jørgensen, "Tensile and compressive properties of cancellous bone," *J. Biomech.*, **24**, 1143–49 (1991).

⁴⁸D.T. Reilly and A.H. Burstein, "Review article—Mechanical properties of cortical bone," *J. Bone Joint Surg. Am.*, **A56**, 1001–22 (1974).

⁴⁹K.J. Koester, J.W. Ager, and R.O. Ritchie, "The true toughness of human cortical bone measured with realistically short cracks," *Nat. Mater.*, **7**, 672–77 (2008).

⁵⁰R. Menig, M. Meyers, M. Meyers, and K. Vecchio, "Quasi-static and dynamic mechanical response of *Haliois rufescens* (abalone) shells," *Acta Mater.*, **48**, 2383–98 (2000).

⁵¹J. Currey, "Mechanical properties of mother of pearl in tension," *Proc. R. Soc. London B, Bio. Sci.*, **196**, 443–63 (1977).■